

# MIXING ENHANCEMENT DUE TO TIME PERIODIC FLOWS IN A T-SHAPED MICRO-MIXER

Chiara Galletti, Elisabetta Brunazzi, Roberto Mauri

*Laboratory of Multiphase Reactive Flows,  
Department of Civil and Industrial Engineering  
Università di Pisa, I-56126 Pisa, Italy*

**Abstract.** A Direct Numerical Simulation of the mixing process between two streams having the same flow rate in a T-shaped micro-device indicates that for a certain range of Reynolds numbers,  $Re$ , the flow regime might be unsteady, with time-periodic structures. Using a rectangular cross section with a 3:2 aspect ratio at the outlet and assuming fully developed flow at the inlet, pulsating flows are observed when  $230 < Re < 410$ ; for example, when  $Re = 360$ , the time periodic structures were characterized by a Strouhal number,  $St \cong 0.25$ , in good agreement with recent experimental results. Predictably, these pulsating flows strongly enhance the degree of mixing, that can be as large as twice the one that is measured in the steady engulfment regime. Then, when we increase the Reynolds number beyond the pulsating range, the flow is no more unsteady, with a consequent reduction of the mixing efficiency. In addition, we also observe that for our investigated geometry the unsteady, periodic behavior does not occur when the inlet flow profiles are blunt and not fully developed.

**Keywords:** Flow instability; Laminar flow; Direct numerical simulation.

## 1. INTRODUCTION

Effective mixing in small volumes is a crucial step in many processes, such as miniature fuel cells, molecular diagnostics and, in general, micro-reactors, where a fast homogenization of reactants is required. Typical uses of microfluidic devices require these systems to be inexpensive and simple to operate, such as passive micro-mixers, where mixing is promoted by stretching and recombining of the flow fields without the help of any external power source [1].

One of the simplest designs of passive micro-mixers is a T shape, in which the inlets join the main channel with T-shaped branches. This type of mixer is also suitable for carrying out fundamental studies, as the T-shaped micro-mixer is often encountered as a junction element in more complex micro-systems. The efficiency of T-shaped micro-mixers for liquid mixing has been largely proved in literature [2].

So far, different flow regimes have been identified in the T-shaped micro-mixer depending on the Reynolds number,  $Re$ , namely: the stratified, the vortex and the engulfment flow regimes [3][4][5][6]. In the stratified flow regime, the inlet streams come into contact in the mixing zone and then flow side by side through the mixing channel, resulting in a completely segregated flow. In the vortex regime, above a critical  $Re$ , a secondary flow in the form of a double vortex pair occurs, due to the instabilities induced by the centrifugal forces at the confluence, leaving however the two incoming streams well segregated. In the engulfment regime, occurring at higher  $Re$ , fluid elements reach the opposite side of the mixing channel, thus largely increasing the degree of mixing. Moreover, for specific  $Re$  ranges above the engulfment, but still in the laminar regime, some kinds of instabilities have been recently observed. For example, based on numerical simulations on a T-mixer with a 2:1 aspect ratio (i.e. the ratio between width,  $W$ , and height,  $H$ , of the mixing channel), Bothe et al. [5] reported that when  $Re > 240$ , thereby above the onset of engulfment occurring at  $Re$

$= 146$ , the flow exhibits a periodic behavior. For T-shaped micro-mixers having the same 2:1 aspect ratio, Dreher et al. [7] investigated, both numerically and experimentally, the flow behavior above the engulfment point, confirming that when  $Re > 240$  the steady state simulations do not converge and transient ones should be adopted instead. According to these authors, this was due to a periodic behavior of the flow; in particular, they identified a periodic pulsating flow for  $240 < Re < 400$ , characterized by a Strouhal number  $0.15 < St < 0.29$ . Such periodic pulsations were found to disappear for larger  $Re$ , i.e. when  $Re > 500$ , where a chaotic, pseudo-turbulent motion was observed. Importantly, such instabilities do enhance the mixing process: indeed, optimum mixing is reached for  $240 < Re < 700$ . An experimental evidence of the occurrence of such flow instabilities was provided also by Thomas et al. [8][9], who investigated through planar and discrete-point Laser Induced Fluorescence the water flow in a T-shaped channel with  $W = 2W' = 40 \text{ mm}$  and  $H = 20 \text{ mm}$  for  $56 < Re < 422$ .

The present work shows results from the Direct Numerical Simulation of a T-shaped micro-mixer, characterized by a different aspect ratio than the one used by previous investigators [5][7][8][9]. Considering a wide range of Reynolds numbers, we investigate when flow instabilities occur, together with their relevance for mixing. Moreover, the effect of the inlet flow conditions on the onset of instability is discussed, as understanding factors affecting this phenomenon may help to optimize and control mixing.

## 2. TEST CASE AND NUMERICAL MODEL

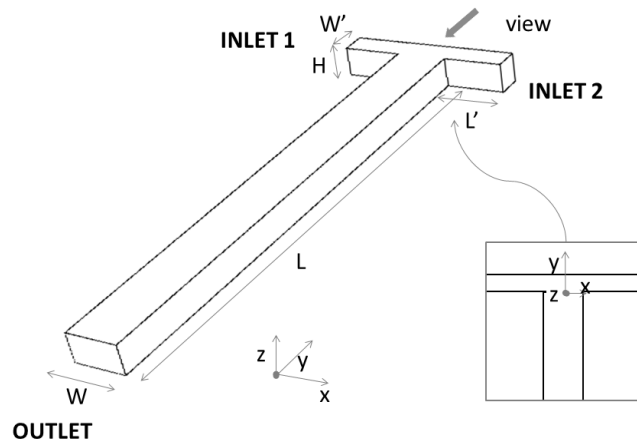


**Figure 1** - Sketch of the T micro-mixer.

In the micro-mixer that we have considered (see figure 1) the mixing channel has a rectangular cross section with a 3:2 aspect ratio (i.e. width  $W = 3H/2$  and depth  $H$ ), with length  $L = 15H$ , while the inlet channels are identical, with a 3:4 aspect ratio (i.e. width  $W' = 3H/4$  and depth  $H$ ) and length  $L' = 7H/4$ . Consequently, as we assume that the two inlet streams have equal flow rates, the mean velocity  $U$  at the inlets is equal to that in the mixing channel; in addition, flow rates were varied so that  $Re$  in the mixing channel ranges from 100 to 530, with the Reynolds number,  $Re = \rho U d / \mu$ , defined in terms of the hydraulic diameter,  $d = 6H/5$ , while  $\rho$  and  $\mu$  are the fluid density and viscosity, respectively. In a parallel experimental work, we use a T-mixer having  $H = 200 \mu\text{m}$ , with mean velocities,  $U$ , ranging from 0.4 to 2.2 m/s.

Simulations were performed using the commercial software Ansys 13, using the FLUENT fluid dynamics package, where length, velocity, time and pressure were scaled in terms of  $d$ ,  $U$ ,  $d/U$  and  $\rho U^2$  [10], i.e.  $y^* = y/d$ ,  $u^* = u/U$ ,  $t^* = tU/d$  and  $P^* = P/\rho U^2$ .

Mixing fluids are assumed to consist of the same Newtonian liquid, i.e. incompressible and with constant viscosity, flowing at constant temperature, so that the governing equation is the Navier-Stokes equation, with a divergence-free velocity field, i.e.,

$$\frac{\partial \mathbf{u}}{\partial t} + \mathbf{u} \cdot \nabla \mathbf{u} + \nabla P = \frac{1}{\text{Re}} \nabla^2 \mathbf{u}; \quad \nabla \cdot \mathbf{u} = 0,$$

where the asterisks have been dropped for convenience.

In the following,  $c$  will be used to denote the normalized concentration (i.e. ranging from 0 to 1) of one of the two inlet streams, or that of a passive tracer. Constant, e.g., ambient, pressure is set at the outlet of the mixing channel, while no-slip boundary conditions are applied to the walls. Velocity boundary conditions are set at both inlets assuming a fully developed velocity profile in a rectangular conduit. This can be determined by solving the Navier-Stokes equations with no-slip boundary conditions at the walls and with constant axial pressure gradient  $G$  [11][12], obtaining,

$$u(y, z) = -\frac{1}{2} \text{Re} Y^2 G \left\{ \frac{y}{Y} \left( 1 - \frac{y}{Y} \right) + \frac{8}{\pi^3} \sum_{k \text{ odd}} \frac{1}{k^3} \sin \left( k\pi \frac{y}{Y} \right) \left[ \text{Cosh} \left( k\pi \frac{z}{Y} \right) - \text{Tanh} \left( \frac{k\pi}{2\eta} \right) \text{Sinh} \left( k\pi \frac{z}{Y} \right) \right] \right\}$$

where  $Y$  and  $Z$  are the non-dimensional sizes of the conduit ( $W'/d$  and  $H/d$  in our case), while  $\eta = W'/H$  is the conduit aspect ratio. The constant pressure gradient  $G$  (in  $\rho U^2/d$  units) can be derived as a function of the Reynolds number as,

$$G = -\frac{12}{Y^2 \text{Re}} \left[ 1 - \frac{192}{\pi^5} \eta \sum_{k \text{ odd}} \frac{1}{k^5} \text{Tanh} \left( \frac{k\pi}{2\eta} \right) \right]^{-1}.$$

After a careful grid independence study on the velocity fields (Galletti *et al.* [13]), a structured grid with regular cubical elements of  $H/50$  size was chosen, corresponding to  $3.3 M$  elements. In particular, there are  $76 \times 50$  elements in each cross section within the mixing channel, thus in agreement with the recommendation by Hussong *et al.* [14].

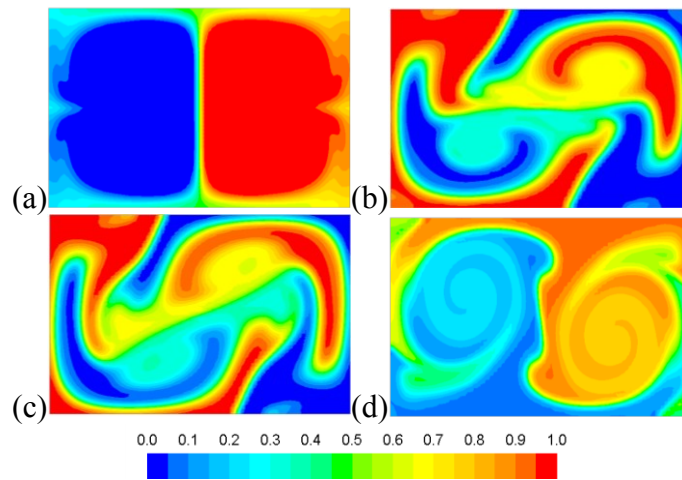
A second order discretization scheme was used for all equations, as higher order solvers were found to provide negligible corrections, thereby ruling out the influence of numerical diffusion. When a steady solver was used, a sufficient number of iterations were performed in order to obtain residuals of less than  $10^{-13}$  for all equations. Transient simulations were performed with an explicit solver, instead, choosing a discretization time step  $\Delta t$  ensuring a Courant number lower than 1, which, in non-dimensional units, yields:

$$\Delta t < \frac{1}{60 U_{mx}},$$

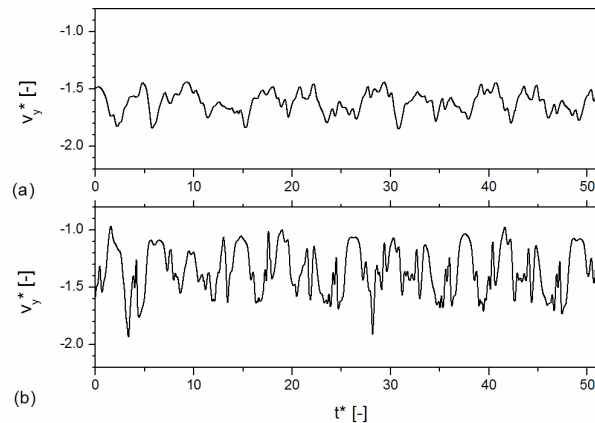
where  $U_{mx}$  is the maximum fluid velocity (in general,  $U_{mx} \cong 2$ ). For instance, using a T-mixer with  $H = 200 \mu\text{m}$  and a water flow with  $Re = 360$  (i.e., with  $U = 1.5 \text{ m/s}$ ), the time step results to be  $5 \times 10^{-7} \text{ s}$ , corresponding to a maximum Courant number within the domain equal to 0.94.

### 3. RESULTS

Figure 2 shows the tracer distribution in the mixing channel cross-section at  $y = -L/3$  for different  $Re$ . Figure 2a refers to  $Re = 144$  in the vortex flow regime, and indicates a poor mixing. Figures 2b and 2c show the engulfment regime ( $Re = 192$  and  $216$ , respectively), characterized by non-symmetrical vortical structures resulting in enhanced mixing. Finally, figure 2d refers to  $Re = 480$ : in this case, it can also be observed the presence of vortical structures, although the pattern is different from those at lower  $Re$ . For all such conditions, a solution could be found with a steady solver. In particular, the  $Re = 480$  run was also performed with a transient solver, indicating steady flow. However, for intermediate  $Re$  (ranging, approximately, from  $230$  to  $410$ ), an unsteady behavior was observed. Figure 3 shows an example of velocity time series evaluated through a DNS simulation for  $Re = 360$  at two different locations in the mixing channel.



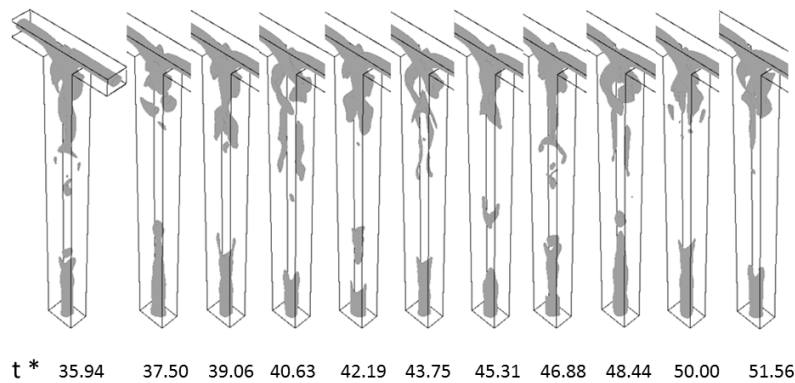
**Figure 2** - Tracer distribution in the mixing channel cross section at  $y^* = -4.17$  (i.e.  $y = -L/3$ ) with (a)  $Re = 144$ ; (b)  $Re = 192$ ; (c)  $Re = 216$  (d)  $Re = 480$ .



**Figure 3** - Time series of the  $y$  component of velocity in the center of the mixing channel at  $Re=360$  for (a)  $y^* = -8.33$  (i.e.,  $y = -2L/3$ ) and (b)  $y^* = -4.17$  ( $y = -L/3$ ).

A preliminary analysis of the time series indicates a rather periodic behavior, characterized by a Strouhal number,  $St = fd/U \cong 0.25$ , where  $f$  is the leading characteristic frequency,  $f \cong 0.25 U/d$ . This result is in excellent agreement with the experimental finding by Dreher *et al.* [7] who, using stroboscopic imaging, measured a similar Strouhal number,  $0.2 < St < 0.25$  for  $270 < Re < 380$ , in a T-mixer with  $W = 2W' = 2H = 600 \mu m$ . Similar results were obtained by Thomas and Ameal [9], who measured a periodic behavior with  $0.11 < St < 0.30$  for  $195 < Re < 298$ , applying laser-induced fluorescence (LIF) techniques to capture the flow dynamics in a larger ( $W = 2H = 40mm$ ) mixing channel.

A more detailed frequency analysis is currently being performed, based on using a pseudo-spectral, highly parallelized CFD code to determine much longer time series. Preliminary results indicate the presence of several frequencies,  $f$  being the dominant among them, although further work is required to reach a final conclusion on this subject.



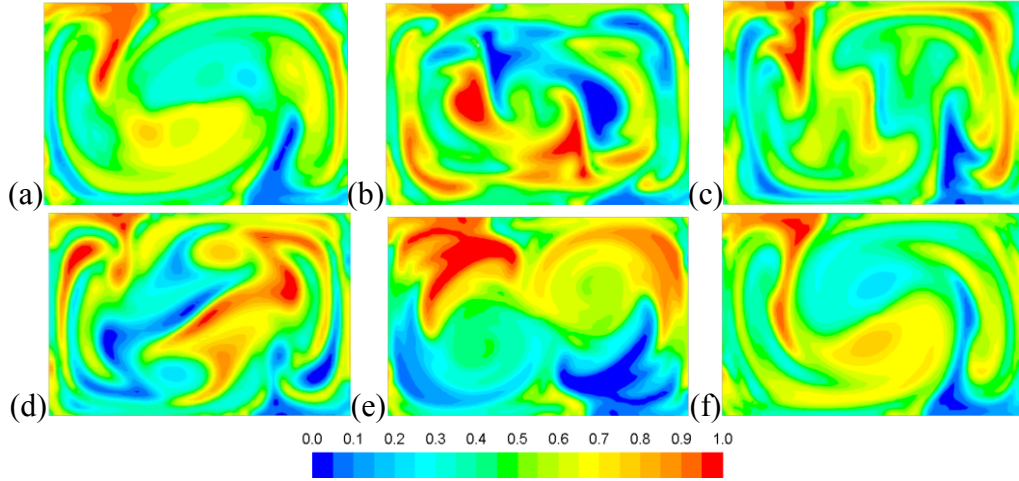
**Figure 4** - Regions of the micro-mixer having velocity  $u > 1.67 U$ , at  $Re = 360$ .

Figure 4 shows the region of the T-mixer where the local velocity is above  $5/3$  of the mean value (i.e.  $u^* > 1.67$ ), evaluated every  $\Delta t^* = 0.56$  time interval (i.e.,  $0.25 ms$  when  $H = 200 \mu m$ ), in order to describe the unsteady flow behavior. Pulsating structures originating from the interaction between the inlet streams can be observed. Consequently, the tracer distribution along the mixing channel varies greatly with time, as depicted in figure 5 for the cross-section located at one third of the length of the mixing channel (i.e. at  $y^* = -4.17$ ). At first glance it can also be noticed that the degree of mixing is larger than that observed for all the  $Re$  of figure 2, being the extension of the green region larger.

Quantitatively, the mixing efficiency is evaluated through the bulk concentration (cup mixing concentration), that is the flow-weighted mean concentration, i.e.:

$$\bar{c} = \frac{\langle cu \rangle}{\langle u \rangle}; \quad \langle cu \rangle = \frac{1}{A} \int_A cudA; \quad \langle u \rangle = \frac{1}{A} \int_A udA, \quad (5)$$

where the overbar indicates the cup mixing average, while the brackets denote the volume (i.e. un-weighted) average on a cross section of area  $A$ . The cup mixing average is preferred over the more usual volume average concentration, because it describes the concentration that “one would measure if the tube were chopped off and if the fluid issuing forth were collected in a container and thoroughly mixed” [15].



**Figure 5** - Tracer distribution in the mixing channel cross-section when  $Re = 360$  at  $y^* = -4.17$  (i.e.,  $y = -L/3$ ) and at different times, (a)  $t^* = 42.19$ ; (b)  $t^* = 43.75$ ; (c)  $t^* = 45.31$ ; (d)  $t^* = 46.88$ ; (e)  $t^* = 48.44$ ; (f)  $t^* = 50$ .

In the same way, a bulk, or cup mixing, mean square concentration difference is defined as:

$$\overline{(\Delta c)^2} = \frac{\langle (c - \bar{c})^2 u \rangle}{\langle u \rangle}; \quad \sigma_{cm}^2 = \overline{(\Delta c)^2} / (\Delta c)_{\max}^2, \quad (6)$$

where the maximum value of the mean square concentration difference is used as a normalizing factor. Clearly, as the maximum mean square concentration difference occurs when the two streams are completely unmixed (i.e.,  $c = 0$  in half of the cross section and  $c = 1$  in the other half), then  $(\Delta c)_{\max}^2 = 1/4$ . For sake of convenience, here the following definition of degree of mixing will be used:

$$\delta_m = 1 - \sigma_{cm} \quad (5)$$

as it varies from 0, when the two streams are perfectly unmixed, to 1, when they are completely mixed.

Figure 6 shows the degree of mixing along the mixing channel evaluated for different flow regimes. In the vortex regime, the degree of mixing is very low (4% maximum) indicating a segregated flow. In the engulfment regime, mixing is enhanced with degree of mixing at the outlet equal to 35% when  $Re = 192$ , and 42% when  $Re = 216$ . The unstable regime is indicated by the black symbols, each of them calculated for different time steps; the unsteady structures originate values of the degree of mixing that are well above those observed for the steady flow conditions. For instance, in the outlet section, the mixing degree varied from 70 to 82% when  $Re = 360$ . Similarly, also pressure drops in the T-mixer were found to vary significantly (i.e. of about 12%) in the unstable regime for  $Re = 360$ .

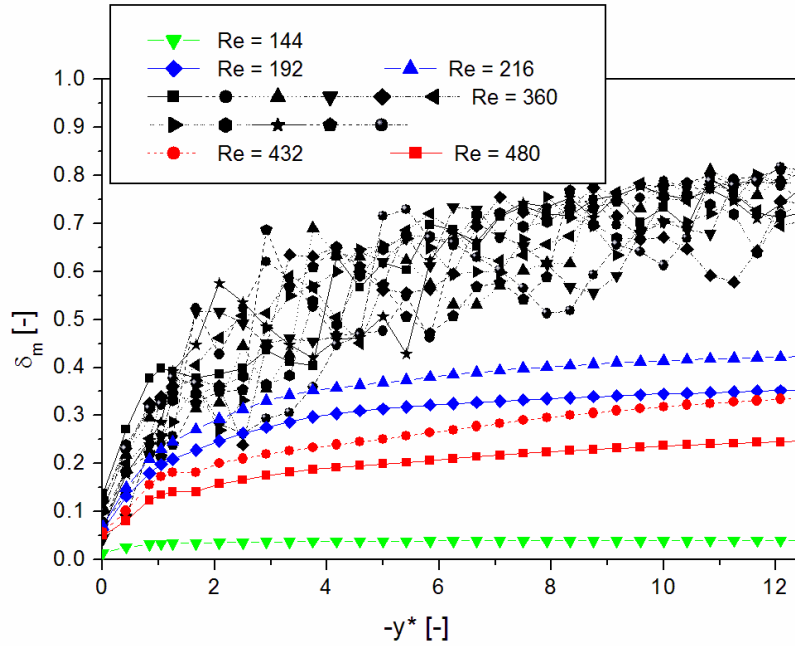


**Figure 6** - Degree of mixing along the mixing channel for different regimes: vortex flow regime (green symbols); engulfment flow regime (blue symbols); unstable flow regime (black symbols); steady flow regime for high  $Re$  (red symbols).

As  $Re$  is increased further, the flow field returns to be steady and the degree of mixing decreases to values that are comparable with those observed in the engulfment regime. For instance, when  $Re = 480$ , we find that at the outlet the degree of mixing is  $\delta_m \cong 25\%$ , which is lower than the value (i.e.  $\delta_m \cong 40\%$ ) at  $Re = 200$ , due to the lower residence time in the mixing channel caused by the larger mean velocity. This result seems in agreement with the experimental measurements by Thomas *et al.* [8], who found that, while for  $136 < Re < 334$  the degree of mixing steadily increases, due to time periodic flow structures, at higher  $Re$  a degree of symmetry is regained and mixing decreases. On the other hand, Dreher *et al.* [7] observed the appearance of a chaotic motion above the pulsating flow regime. This apparent disagreement could be due to either the different aspect ratio or, more probably, to the stabilizing effect of the longer mixing channel that we have used.

Finally, it should be stressed that the appearing of an unsteady, pulsating regime depends not only on the geometric characteristics of the device and the operating Reynolds number, but also on the type of flow conditions at the inlets. In fact, Galletti *et al.* [13] and, more recently Fani *et al.* [16], showed that flow instabilities occur only when the velocity profile at the inlet is peaked and therefore do not appear when, for example, the inlet flow is not fully developed (i.e. the inlet channels are not long enough to ensure that fully developed flow conditions are reached).

## 5. CONCLUSIONS

An unsteady flow regime is observed for  $Re$  ranging from 230 to 410 in a T-shaped micro-mixer having a rectangular cross section with a 3:2 aspect ratio at the outlet, thus confirming the findings by Dreher *et al.* [7] and Thomas *et al.* [8][9], who nevertheless used different aspect ratios. The unsteady flow is characterized by pulsating structures, which strongly enhance mixing, leading to values of the degree of mixing that are almost twice as

large as those achieved in the engulfment flow regime. For larger  $Re$ , above the unsteady flow regime, a steady flow was observed again, with a strong reduction of the mixing efficiency. Therefore, the precise knowledge of the operating conditions for which the unstable flow occurs, are of great importance for micro-mixer optimization. Moreover, the instabilities may be enhanced or damped by specific conditions: for instance, Fani et al. [16] showed that non-fully developed velocity profiles at the inlets may suppress all unstable flows.

### Acknowledgment

This work was supported in part by the Italian Ministry of Education and Research (MIUR), grant PRIN, No. 2009-3JPM5Z.

### REFERENCES

- [1] V. Kumar, M. Paraschivoiu, K.D.P. Nigam, Single-phase fluid flow and mixing in microchannels, *Chem. Eng. Sci.* 66 (2011) 1329-1373.
- [2] D. Bökenkamp, A. Desai, X. Yang, Y. Tai, E. Marzluff, S. Mayo, Microfabricated silicon mixers for submillisecond quench-flow analysis, *Anal. Chem.* 70 (1998) 232–236.
- [3] M. Hoffmann, M. Schlüter, N. Rübiger, N., Experimental investigation of liquid–liquid mixing in T-shaped micro-mixers using  $\mu$ -LIF and  $\mu$ -PIV, *Chem. Eng. Sci.* 61 (2006) 2968-2976.
- [4] M. Engler, N. Kockmann, T. Kiefer, P. Woias, Numerical and experimental investigations on liquid mixing in static micromixers, *Chem. Eng. J.* (2004) 315-322.
- [5] D. Bothe, C. Stemich, H.-J. Warnecke, Fluid mixing in a T-shaped micro-mixer, *Chem. Eng. Sci.* 61 (2006) 2950-2958.
- [6] N. Kockmann, D.M. Roberge, Transitional flow and related transport phenomena in curved microchannels, *Heat Transfer Engineering* 32 (2011) 595-608.
- [7] S. Dreher, N. Kockmann, P. Woias, Characterization of laminar transient flow regimes and mixing in T-shaped micromixers, *Heat Transfer Eng.* 30 (2009) 91-100.
- [8] S. Thomas, T.A. Ameel, J. Guilkey, Mixing kinematics of moderate Reynolds number flows in a T-channel, *Phys. Fluids* 22 (2010) 013601 (10 pp).
- [9] S. Thomas, T.A. Ameel, An experimental investigation of moderate Reynolds number flow in a T-Channel, *Exp Fluids* 49 (2010) 1231–1245.
- [10] J.M. Ottino, S. Wiggins, Introduction: mixing in microfluidics, *Philos. Trans. R. Soc. London, Ser. A* 362 (2004) 923-935.
- [11] P.C. Chatwin, P.J. Sullivan, The effect of aspect ratio on the longitudinal diffusivity in rectangular channels, *J. Fluid Mech.* 120 (1982) 347-358.
- [12] J. Happel, H. Brenner, *Low Reynolds Number Hydrodynamics*, Prentice Hall, New York, 1965 (Eq. 2-5.24).
- [13] C. Galletti, M. Roudgar, E. Brunazzi, R. Mauri, Effect of inlet conditions on the engulfment pattern in a T-shaped micro-mixer, *Chem. Eng. J.* 185–186 (2012) 300-313.
- [14] J. Hussong, R. Lindken, M. Pourquie, J. Westerweel, Numerical study on the flow physics of a T-shaped micro mixer, in: *IUTAM Symposium on Advances in Micro- and Nanofluidics* (B.V. M. Ellero et al., eds), IUTAM Bookseries 15, Springer Science, New York, 2009.
- [15] R.B. Bird, W.E. Stewart, E.N. Lightfoot, *Transport Phenomena*, Wiley, New York, 1960 (pp. 297 and 641).
- [16] A. Fani, S. Camarri, C. Galletti, E. Brunazzi, M.V. Salvetti, R. Mauri, Sensitivity of the engulfment to inlet flow conditions in a T-shaped micro-mixer: CFD and perturbation analysis, *Proc. 3rd Eur. Conf. on Microfluidics*, Heidelberg, (2012).